Available online at www.sciencedirect.com
ScienceDirect
Journal of Nuclear Materials 373 (2008) 429–432
journal of nuclear materials
www.elsevier.com/locate/jnucmat

Letter to the Editors

Corrosion and microstructural characteristics of Zr–Nb alloys with different Nb contents

Hyun Gil Kim [a,*], Sang Yoon Park [a], Myung Ho Lee [a], Yong Hwan Jeong [a], Sun Doo Kim [b]

[a] *Advanced Core Materials Lab, Korea Atomic Energy Institute, Yuseong-gu, Daejeon 305-600, South Korea*
[b] *Korea Nuclear Fuel Co. Ltd., Yuseong-gu, Daejeon 305-353, South Korea*

Received 17 May 2006; accepted 4 May 2007

Abstract

To improve their corrosion resistance and mechanical properties, Nb is added to most of the advanced Zr-based alloys. So, in this study, a systematic investigation was performed on Zr–*x*Nb alloys ($x = 0.1$–2.0 wt%) to establish the optimized Nb content and annealing temperatures which were applied during manufacturing process. A corrosion resistance of Nb-containing Zr alloys was considerably affected by the Nb content as well as annealing temperature. The good corrosion resistance was obtained when the Nb content was controlled to be 0.2–0.3 wt% and the annealing temperature of the high Nb-containing alloys during the manufacturing process was performed at 570 °C. From the microstructural investigations by using TEM/EDS, the corrosion resistance was controlled by the Nb solubility in alpha Zr and the type of β-phases which were determined by the annealing temperature.

1. Introduction

Zr-based alloys are being used as fuel cladding and structural materials for nuclear reactors, since these alloys have a good irradiation stability, corrosion resistance, and mechanical properties in a reactor environment. Recently, more advanced Zr-based alloys have become necessary for enhanced operating conditions such as an increased burn-up and higher operation temperatures [1–4]. The tendency that Nb was selected as a major alloying element in the Zr-based alloy is a common characteristic for the newly developed fuel claddings. So, it is necessary to investigate the effect of the Nb-content and the effect of an annealing after a beta quenching on the corrosion of Zr–*x*Nb binary alloys, for developing advanced nuclear fuel cladding materials with an improved corrosion resistance.

The investigation on the corrosion behavior as well as the phase transformation of Zr–Nb alloys have been performed by many researchers. Some of them have reported that the Zr alloys containing a low Nb content showed a good corrosion resistance [5,6]. From a study of the effect of the β phase on a corrosion, it has also been reported that corrosion rate of Zr–Nb alloy increased with the formation of the β_{Zr} phase but it decreased with the formation of the β_{Nb} phase [7–9]. Especially, the solid solution effect of Nb-content and the type and fraction of β_{Zr} phase on corrosion were systemically studied for the water quenched and annealed Zr–Nb alloys [8]. The correlation between the microstructural properties such as Nb-content, type of precipitates and oxide characteristics was studied for the Zr–*x*Nb alloys which were isothermally annealed at 570 and 640 °C [9]. As such, the corrosion rate of Nb-containing Zr alloys is known to depend on the Nb content in the matrix and the type of β-phases.

However, the corrosion behavior of the Zr–*x*Nb alloys which were manufactured by the application of different annealing temperature during cold working process was not classified in the previous studies. So, the corrosion behavior of Zr–*x*Nb alloys having different manufacturing process was investigated in this work.

* Corresponding author. Tel.: +82 42 868 2522; fax: +82 42 862 0432.
E-mail address: hgkim@kaeri.re.kr (H.G. Kim).

0022-3115/$ - see front matter © 2007 Elsevier B.V. All rights reserved.
doi:10.1016/j.jnucmat.2007.05.035

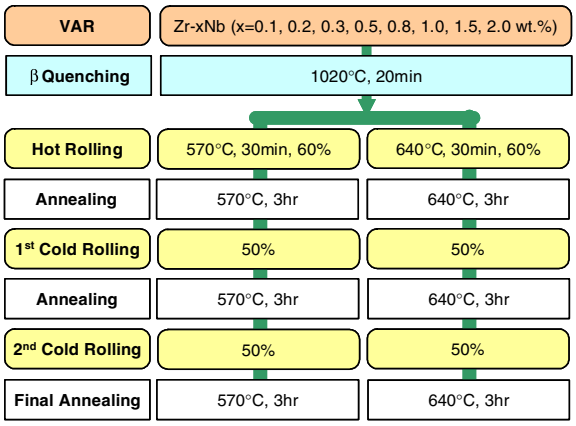

Fig. 1. Chemical composition and manufacturing process of the Zr–*x*Nb alloys.

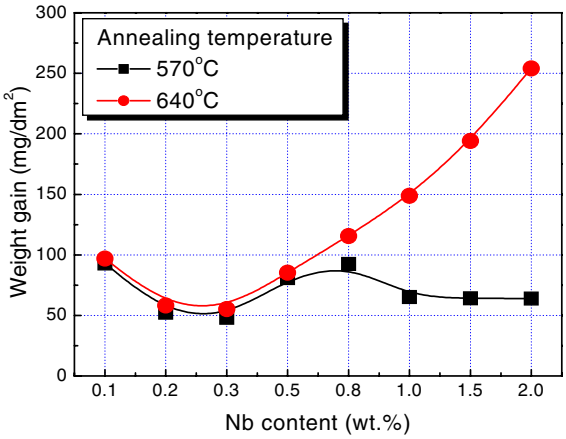

Fig. 2. Corrosion behaviors of the Zr–*x*Nb alloys with the Nb content and annealing temperature corroded at 360 °C for 150 days.

2. Experimental procedure

The alloys containing 0.1–2.0 wt% Nb were prepared by the manufacturing process shown in Fig. 1. The alloy was prepared by the vacuum arc remelting method with sponge zirconium and high purity (99.99%) niobium and then this ingot was β solution treated at 1020 °C for 20 min. The quenched ingot was hot-rolled after a pre-heating at 570 °C and 640 °C for 30 min and cold-rolled two times to a final thickness of 0.8 mm. Between the rolling steps, the cold-rolled sheet was intermediate-annealed at 570 °C and 640 °C for 3 h.

Samples for the corrosion test, 25 by 20 by 0.8 mm in size, were cut from the manufactured strip, mechanically ground up to 1200 grit SiC paper, and then pickled in a solution of 5 vol.% HF, 45 vol.% HNO_3 and 50 vol.% H_2O. The final thickness of the corrosion test samples after pickling was 0.56 mm. The corrosion test was performed in a static autoclave with distilled water under the condition of 360 °C and 18.9 MPa according to the procedure of ASTM G2-88. The corrosion behavior were evaluated by measuring the weights gains of the corroded specimens. The microstructure observation and the precipitates analysis of the samples were performed by using a transmission electron microscope (TEM) equipped with EDS.

3. Results and discussion

3.1. Corrosion behaviors

Fig. 2 shows the results of the corrosion test of the Zr–*x*Nb alloys tested at 360 °C for 150 days. It was observed that the corrosion behaviors of the Zr–Nb binary alloys were quite different depending on the Nb content and the intermediate annealing temperature during the manufacturing process. The corrosion behavior of the Zr–*x*Nb alloys was changed with the Nb content and the intermediate annealing temperature. The corrosion behavior of the low Nb containing alloys in the range of 0.1–0.8 wt% were very similarly regardless of the annealing temperature of 570 °C and 640 °C. As the Nb content increased, the weight gain was decreased up to about 0.3 wt% Nb, and it was increased with an increasing Nb content up to 0.8 wt% in both samples annealed at 570 °C and 640 °C. However, in the range of a high Nb content from 1.0 to 2.0 wt%, the corrosion rate of the alloys was considerably changed with the annealing temperature. The corrosion rate of the sample annealed at 570 °C was much lower than that of the sample annealed at 640 °C, and the corrosion rate of the sample annealed at 640 °C was considerably increased with Nb content. This result of the corrosion behavior is similar to the previous result [9] which is studied for the isothermal annealing effect after β-quenching of Zr–*x*Nb alloys.

3.2. Microstructure characteristics

Fig. 3 shows the TEM micrographs of the second phase particles of Zr–*x*Nb alloys with the annealing temperature. The type and volume fraction of the second phase particle were changed by increasing the Nb content and annealing temperature. In the Zr–0.2Nb alloy annealed at 570 °C and 640 °C, the second phase particle of a small size was observed and the type of the second phase particle was revealed as a Zr_3Fe precipitate by using the TED/EDS and SAD analysis. The formation of a Zr_3Fe type precipitate resulted from the Fe as an impurity contained in the zirconium. In the range of 0.8–2.0Nb of the alloys, the type and size of the second phase particles in the sample were clearly changed by the annealing temperature. In the alloys annealed at 570 °C, $Zr(NbFe)_2$ type precipitates were mainly observed in the matrix of the Zr–0.8Nb alloy and a β_{Nb} phase was mainly observed in the matrix of the Zr–1.0Nb, Zr–1.5Nb and Zr–2.0Nb alloys. In the alloys annealed at 640 °C, $Zr(NbFe)_2$ type precipitates were mainly observed in the matrix of the Zr–0.8Nb alloy and the β_{Zr} phase was mainly observed in the matrix of the Zr–1.0Nb, Zr–1.5Nb and Zr–2.0Nb alloys.

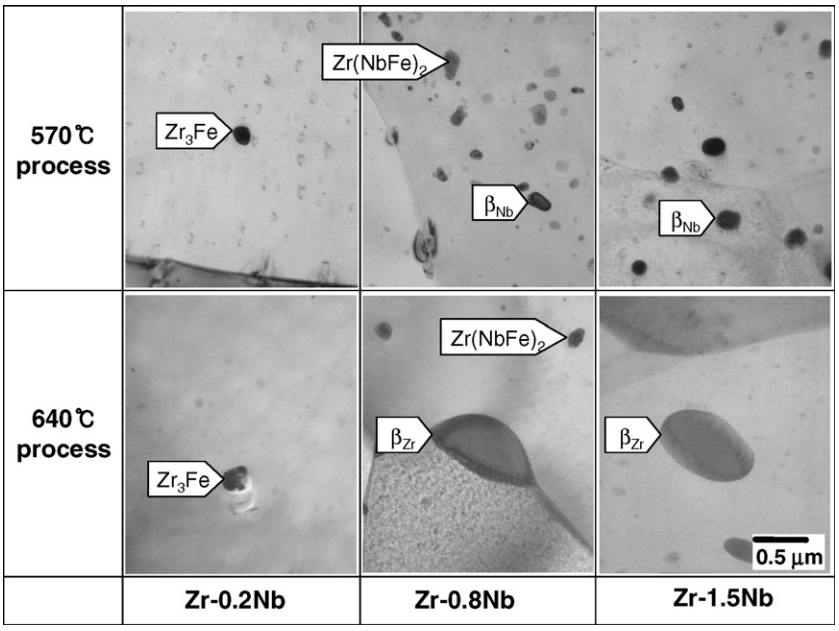

Fig. 3. TEM micrographs of the Zr–*x*Nb alloys annealed at 570 °C and 640 °C with variation of the Nb content.

Table 1 shows a summary of the second phase particles investigated in this study. The characteristics of the second phase were changed with the annealing temperature and Nb content. It was found that the Zr_3Fe precipitate was mainly formed in the low Nb-containing alloys which were lower than 0.3 wt% Nb, and the $Zr(NbFe)_2$ precipitate was also mainly formed in the range of 0.5–0.8Nb of the alloys annealed at both 570 °C and 640 °C. In the high Nb-containing alloys from 1.0 to 2.0 wt%, the β_{Nb} phase was mainly formed in that alloys annealed at 570 °C, however, the β_{Zr} phase was mainly formed in that alloys annealed at 640 °C. The formation of two types of β-phases (β_{Nb} and β_{Zr}) depended on the intermediated annealing temperatures of 570 °C and 640 °C was well matched with previous study for the phase boundary in commercial grade Zr–Nb alloys [10]. The size and volume fraction of the β_{Zr} phase was larger than that of the β_{Nb} phase in an equal Nb content in the high Nb containing alloys. It was caused by the Nb concentration in the β-phases, because the Nb content in β_{Zr} phase was in range from 20 to 50 wt% while that in β_{Nb} phase was more than 90 wt% [11]. Therefore, the type, size and volume fraction of the second phase in the Zr–Nb alloys was determined by the Nb content as well as annealing temperature. In the high Nb-containing alloys annealed at 570 °C, the accumulated annealing time to form the β_{Nb} phase was shown as about 10 h in this study, while that time to form that phase was shown as about 50 h in the previous study which was studied on the effect of the isothermal annealing time at 570 °C after β-quenching of Zr–*x*Nb alloys [12]. So, the β_{Nb} phase in an equal Nb content in the high Nb containing alloys was more quickly formed in this study compared to the previous result [12]. It was assumed that the working process of the one step of hot rolling and the two steps of cold rolling during the

Table 1
Summary of second phase characteristics of Zr–*x*Nb alloys

Process		Nb content (wt%)		
		0.2	0.8	1.5
570 °C Process	Type	■Zr_3Fe	–	–
		–	■$Zr(NbFe)_2$	□$Zr(NbFe)_2$
		–	□β_{Nb}	■β_{Nb}
	Mean diameter (nm)	88	92	95
	Area fraction (%)	<1	2.6	3.9
	Distribution	α-grain and grain-boundary	α-grain and grain-boundary	α-grain and grain-boundary
640 °C Process	Type	■Zr_3Fe	–	–
		–	■$Zr(NbFe)_2$	□$Zr(NbFe)_2$
		–	□β_{Zr}	■β_{Zr}
	Mean diameter (nm)	105	312	341
	Area fraction (%)	<1	5.2	8.7
	Distribution	α-grain and grain-boundary	α-grain and grain-boundary	α-grain and grain-boundary

■: Major particle, □: Minor particle.

specimen manufacturing was acted as a driving force for the precipitation of the β_{Nb} phase.

3.3. Correlation between corrosion and second phase characteristics

The corrosion behavior of Zr–Nb alloy was considerably changed with the Nb content and annealing temperature. From the second phase analysis, it was found that the corrosion rate was correlated with the Nb concentration in the matrix, precipitate and β phase. In the range of a low Nb content from 0.1 to 0.3 wt%, the weight gain slightly decreased. The Nb-containing precipitate and β phase were not observed by using a TEM observation and the corrosion rate was not affected by the annealing temperature in this Nb-containing region. Therefore, it is assumed that the corrosion rate would be controlled by the soluble Nb in the matrix. In the range of a medium Nb content from 0.5 to 0.8 wt%, the weight gain increased with the Nb content. Since the Nb-containing precipitate was formed in this Nb-containing range, it is considered that the corrosion rate would be controlled by the Nb-containing precipitate which was increasing the corrosion rate. In the range of a high Nb from 1.0 to 2.0 wt%, the corrosion rates were considerably changed by the annealing temperature. The corrosion rate of the sample annealed at 570 °C with a formation of the β_{Nb} phase was much lower than that of the sample annealed at 640 °C with a formation of the β_{Zr} phase. The corrosion rate was not changed with the volume fraction of the β_{Nb} phase, however, it was sharply increased by increasing the volume fraction of the β_{Zr} phase.

4. Conclusion

The corrosion behavior and microstructural characteristics of Zr–*x*Nb alloys were different depending on the Nb content and annealing temperature during the manufacturing process. In the low Nb content of 0.2–0.3 wt%, where Nb was soluble in the matrix without the formation of Nb-containing precipitates or the β phase, the alloys showed a good corrosion resistance and their corrosion resistance was not affected by the annealing temperature. In the middle range Nb content of 0.5–0.8 wt%, where a Nb-containing precipitate was formed in the matrix, the corrosion resistance was increased by increasing the Nb content. In the high Nb content of 1.0–2.0 wt%, the corrosion rate was sensitive to the type of the β phase which was determined by the annealing temperature.

Acknowledgements

This study was supported by Korea Institute of Science and Technology evaluation and planning (KISTEP) and Ministry of Science and Technology (MOST), Korean government, through its national nuclear technology program.

References

[1] G.P. Sabol, G.R. Kilp, M.G. Balfour, E. Roberts, ASTM STP 1023 (1989) 227.
[2] A.V. Nikulina, Y.K. Bibilashvili, P.P. Markelov, M.M. Peregu, V.A. Koterekhov, A.F. Lositsky, N.Y. Kuzmenko, Y.P. Shevnin, V.K. Shamardin, G.P. Kobylyansky, A.E. Novoselov, ASTM STP 1295 (1996) 785.
[3] J.P. Mardon, G. Garner, P. Beslu, D. Charquet, J. Senevat, in: Proceedings of the 1997 International Topical Meeting on LWR Fuel Performance, Portland, Oregon, March 2–6, 405 (1997).
[4] S. Suzuki, K. Murakami, T. Takahashi, in: Proceedings of the 1994 International Topical Meeting on LWR Fuel Performance, West Palm Beach, Florida, April 17–21, 352 (1994).
[5] H.H. Klepfer, J. Nucl. Mater. 9 (1963) 65.
[6] T. Isobe, Y. Matsuo, ASTM STP 1132 (1991) 346.
[7] G.P. Sabol, R.J. Comstock, U.P. Nayak, ASTM STP 1354 (2000) 525.
[8] V.F. Urvanic, M. Griffiths, ASTM STP 1354 (2000) 641.
[9] Y.H. Jeong, H.G. Kim, T.H. Kim, J. Nucl. Mater. 317 (2003) 1.
[10] H.G. Kim, J.Y. Park, Y.H. Jeong, J. Nucl. Mater. 347 (2005) 140.
[11] C.E. Lundin, R.H. Cox, USAEC Report, GENP-4089 1, 1962, p. 9.
[12] H.G. Kim, Y.H. Jeong, T.H. Kim, J. Nucl. Mater. 326 (2004) 125.